J. Electrochem. Sci. Eng. **12(3)** (2022) 557-563; http://dx.doi.org/10.5599/jese.1352

Open Access : : ISSN 1847-9286
www.jESE-online.org

Original scientific paper

Local electrochemical deposition of copper from sulfate solution

Georgii Vasyliev✉, Viktoria Vorobyova, Dmytro Uschapovskiy and Olga Linucheva

National Technical University of Ukraine "Igor Sikorsky Kyiv Polytechnic Institute", 37, Prospect Peremohy, Kyiv-56, 03056, Ukraine

Corresponding author: ✉g.vasyliev@kpi.ua ; Tel.: +38-096-924-9888; Fax: +38-044-204-9773

Received: April 20, 2022; Accepted: May 26, 2022; Published: June 7, 2022

Abstract

Local electrochemical deposition is a type of electroplating used to plate metal locally or form metal objects using electrochemical principles at a short distance from the working electrode. In this work, deposition of the copper spot was modelled using COMSOL software and experimentally tested in copper sulfate electrolyte using soluble copper anode. The working capillary diameter was 4 mm and the interelectrode distance was 5 mm. The deposited copper of 100 µm thickness was investigated using the 3D-profilometry technique. The geometry of deposited metal was found to be in good accordance with the COMSOL model. The inclusions of anodic sludge were responsible for the surface inhomogeneity of the deposited copper.

Keywords

Local electrochemical deposition; additive manufacturing; copper plating; computer modelling; throwing power; anodic sludge

Introduction

Additive manufacturing (AM) is an emerging trend in industry and materials science that provides simple manufacturing of complex objects and opens new approaches in the materials design and manufacturing process. The variety of AM materials becomes wider every year simultaneously with the development of manufacturing techniques. Metal AM is a challenging task due to their high melting temperature. The most industrially developed technique is based on the local melting of metal powder with a laser or electron beam [1,2]. Despite the ability to produce complex objects, the technique requires metal powder preparation and a high energy power source. Electrochemical deposition can be an alternative to the local laser melting because of its low energy consumption (the process takes place at room temperature) and the object is not subjected to temperature influence.

Several electrochemical AM techniques are known today. They can be divided into two main groups, depending on the deposition conditions: mask-based deposition and mask-less deposition [3]. In the former technique, the cathode is covered with the insulating mask covering areas where deposition should not occur. So, the metal deposits on uncovered surfaces [4]. Another mask-based

technique is instant masking plating. In this technique, the mask moves with an anode. The deposition starts only when the mask is attached to the surface. Once the electrolyte is depleted, the depositions stop, the mask is lifted away, and the electrolyte is renewed [5]. Electrochemical fabrication is a manufacturing technique where the deposition of structural material is alternated with the deposition of sacrificial metal, which plays the role of a mask [6]. Once the deposition of the whole structure is completed, the sacrificial metal is etched to obtain the final structure.

Mask-less deposition techniques are carried out with no mask on the surface and the environment around the electrode is open. The first example of this group is localized electrochemical deposition (LECD), proposed in 1995 [7]. The technique is based on the deposition of metal in the localized area under the working electrode. To get a very localized electric field, an ultrafine inert anode tip and small interelectrode gap are used. Further development of the proposed technique was focused on anode construction improvement. The anode was placed inside the dielectric capillary that provides an additional focus of the electric field [8-10].

Jet electrodeposition is another LECD technique, where the impinging anodic electrolyte jet as anode tool to deposit metal selectively deposits metal on the cathode [11]. In meniscus-confined electroplating, the deposition is located in a meniscus-shaped electrolyte bridge between a narrow anode tip and cathode substrate [12-16]. The deposition rate is determined by the diffusion rate of ions and is very low. Extremely small objects can be obtained using fluidic force microscope electrodeposition [17]. In this technique, the hollow AFM cantilever with an aperture at the tip is used. During deposition, the cantilever serves as a working electrode and is filled with electrolyte. The flow of electrolyte from the probe is controlled by pressure regulation. Once the probe is positioned, the deposition starts and ends when the deposited metal touches the tip. Then the probe moves to the next position. Comparing different electrochemical additive manufacturing techniques, it can be seen that the higher precision of manufacturing, the lower the deposition rate. Further investigations are required to develop a highly productive ECAM technique that is able to produce large-scale objects at commercially acceptable rates.

In this work, the local electrochemical deposition of copper was performed using a computer model and compared to electrochemically deposited metal using 3D-profilometry.

Computer modelling

The computer model of the local electrochemical deposition was built using COMSOL Multiphysics 5.2 software. The scheme of the cell is given in Figure 1a. The computer model gives the ability to predict the localization of the electric field and thus the location of the deposited metal. Moreover, the model gives the expected profile of the deposited copper based on the electrical field distribution and deposition duration.

The localization of deposition is highly dependent on the throwing power of the electrolyte. The letter one depends on the conductivity of the solution. The conductivity of the copper plating electrolyte depends on the $CuSO_4$ content, but in technological processes, the sulfuric acid is added. So, the addition of H_2SO_4 increases the conductivity, which makes the distribution of deposited copper more uniform and decreases the voltage load on the plating bath. On the contrary, in this study copper deposition is localized, so the amount of acid should be reduced. To study the influence of H_2SO_4 content on copper local deposition, the calculations were performed for several concentrations.

The COMSOL electrochemical deposit module requires the value of polarizability of the cathodic electrochemical process. The polarizability di/dE was determined experimentally (Figure 2).

Galvanodynamic cathodic polarization curves were obtained using conventional three-electrode cell. The scan rate was 20 mA s^{-1}. The plates of 1×1 cm^2 manufactured from copper grade M0 served as working and auxiliary electrodes, and a saturated silver chloride electrode (SSCE) was used as a reference one (E_{ref} = 0.2 V *vs.* NHE). The potential values on polarization curves are given *vs.* SSCE. Standard electrode potential of copper $E_{Cu^{2+}/Cu}$ = +0.34 V *vs.* NHE or $E_{Cu^{2+}/Cu}$ = +0.14 V *vs.* SSCE, which agrees well with experimental data (Figure 2).

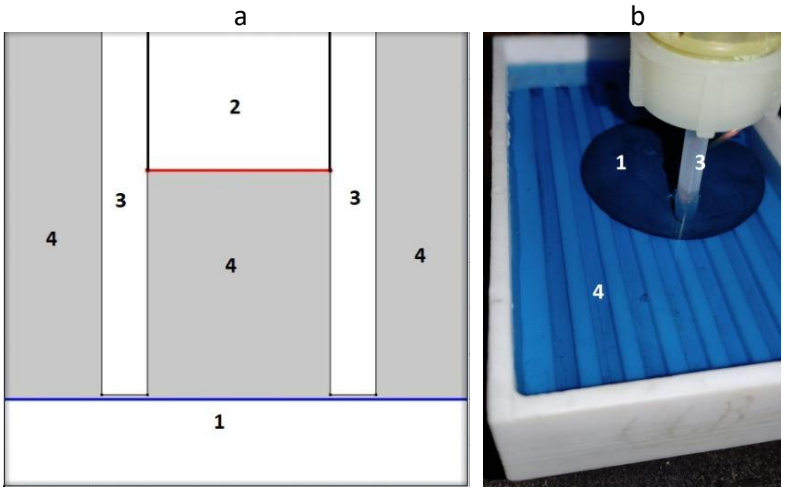

Figure 1. *Scheme (a) and photo (b) of electrochemical cell: 1 – cathode; 2 – anode; 3 – polypropylene tube; 4 – electrolyte*

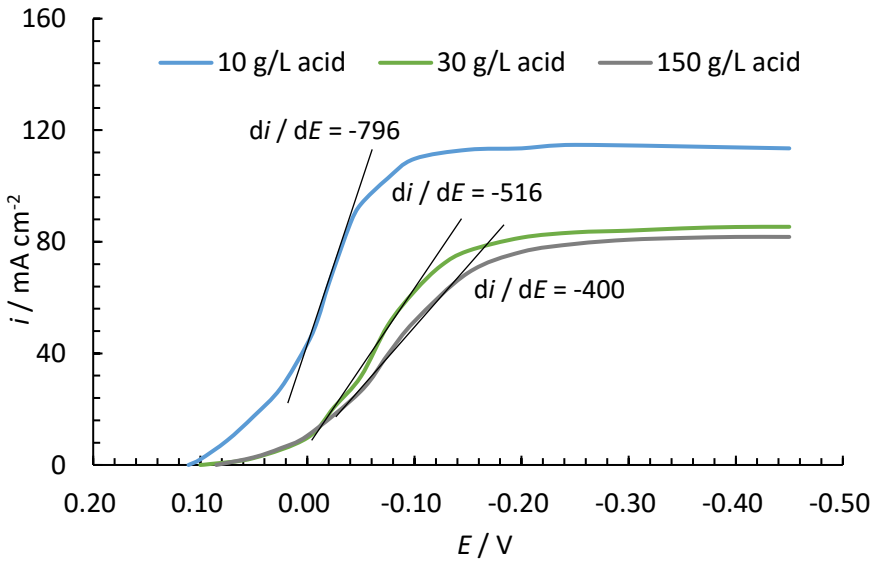

Figure 2. *Cathodic polarization curves of copper deposition in the electrolyte containing 200 g/L $CuSO_4$ and sulfuric acid in different concentrations*

The limiting current density appeared to depend on the sulfuric acid content even in the same concentration of copper ions [18]. This can be explained by the influence of migration part of mass transfer. According to equation (1), the limiting current density, i_L, of copper reduction is dependent on the copper ion transport number:

$$i_L = \frac{2FDC_{Cu^{2+}}}{\left(1-t_{Cu^{2+}}\right)\delta} \quad (1)$$

where D – diffusion coefficient of copper ions, $C_{Cu^{2+}}$ - copper ions concentration, $t_{Cu^{2+}}$ - copper ions transport number, δ - diffusion layer thickness.

The electrolyte solution contains the following ions: H^+, Cu^{2+}, SO_4^{2-} and copper ions transport number can be determined by the equation (2):

$$t_{Cu^{2+}} = \frac{C_{Cu^{2+}} + 2\lambda_{Cu^{2+}}}{C_{Cu^{2+}} + 2\lambda_{Cu^{2+}} + C_{SO_4^{2-}} + 2\lambda_{SO_4^{2-}} + C_{H^+} + 2\lambda_{H^+}} \quad (2)$$

where $\lambda_{Cu^{2+}}$, $\lambda_{SO_4^{2-}}$, λ_{H^+} - are molar conductivity of copper, sulfate, and proton ions. Due to the much higher molar conductivity of protons, the ion transport number of copper will decrease as acid concentration increases, so the limiting current density of copper deposition will decrease as well.

The configuration of the cell is given in Figure 3a. The diameter of the working nozzle was 4 mm, and the copper wire was placed inside it and worked as a soluble anode. The distance between the copper anode and the surface was 5 mm. The gap between the nozzle and the surface was 0.1 mm. The deposition duration was 70 min. The rest of the parameters are given in Table 1.

Table 1. *Copper local deposition modelling parameters*

Parameter	Study number		
	1	2	3
H_2SO_4 content, g L^{-1}	10	30	144
σ / S cm^{-1}	0.050	0.125	0.433
(di / dE) / mA cm^{-2} V^{-1}	796	516	400
φ_{ext} / V	0.82	0.55	0.49

The results of modelling are given in Figure 3b. The growth profiles show that the copper was deposited locally in the form of a cylinder, with a thickness of 100 µm. However, the curvature of the side surface depends on the acid concentration. The closest profile was obtained in the lower tested acid concentration of 10 g L^{-1}. The increase of H_2SO_4 content to 150 g L^{-1} makes the deposited copper spot nearly 2 times wider. So, for experimental testing, the electrolyte with 200 g L^{-1} $CuSO_4$ and 10 g L^{-1} H_2SO_4 was chosen.

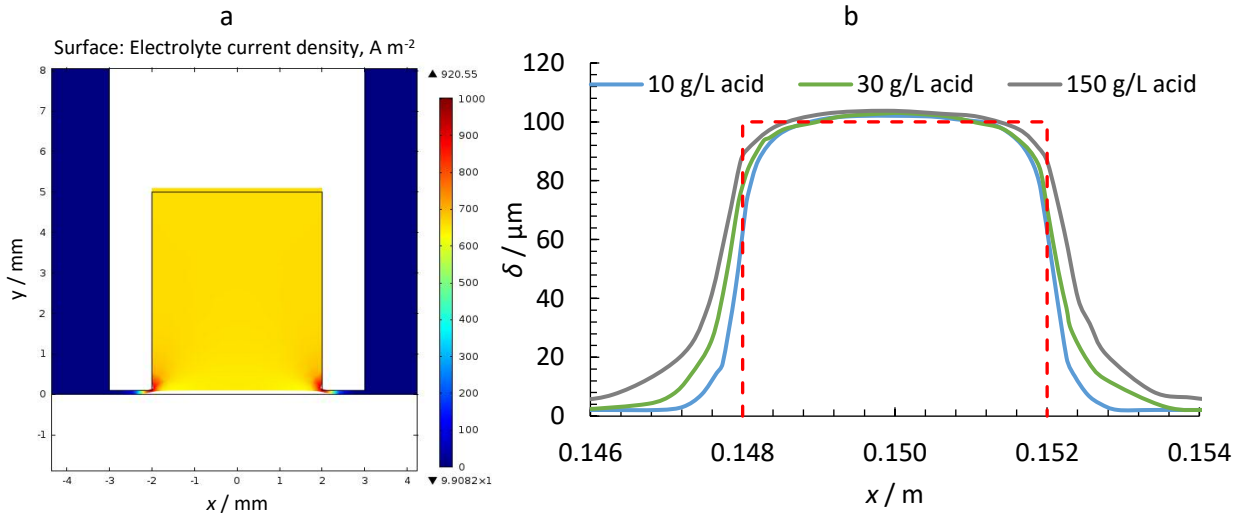

Figure 3. *Current density distribution in the interelectrode area of the cell (a) and the growth profiles of copper (b), modelled for a 0.1 mm gap between the nozzle and the surface in 200 g/L sulfate electrolyte and different sulfuric acid concentrations*

Experimental

The deposition of copper was performed in the same electrochemical cell, consisting of two electrodes (Figure 1b). The same cell configuration was used for computer modelling. The copper

plate was placed at the bottom of the vessel, filled with electrolyte, and attached to the negative pole of the current source. The counter electrode was made from copper wire and placed inside the polypropylene tube of 5×0.5 mm. The tube was oriented in the center of the copper plate and the distance between the plate and the pipe was 5 mm. This arrangement was maintained during the deposition process.

The electrolyte used in the study contained 200 g L^{-1} $CuSO_4$ and 10 g L^{-1} H_2SO_4. Working current density was determined from polarization curves and composed 65 mA cm^{-2}. The height of the deposited copper was set to 100 μm, so the calculated deposition time was 70 min. The electrolysis was performed at ambient temperature.

The characterization of the deposited copper was performed with the 3D-profilometry technique. The sensitive piezoelectric sensor with a vertical resolution of 250 nm/dot and horizontal resolution of 625 nm dot^{-1}, scanned the area of 7×7 mm^2 around the deposited copper spot. The obtained data were collected using a PC and SURFARE software was used to get a 3D image of the surface. The height of the deposited copper, surface roughness and precision of deposition was determined and compared to the COMSOL model.

Results and discussion

Copper deposition is an electrochemical reduction process which undergoes according to equation (3):

$$Cu^{2+} + 2e^- = Cu \quad (3)$$

The rate of copper deposition is determined by the rate of copper supply to the surface, so the working current density was determined experimentally. Figure 2 shows the polarization dependence of copper that was used to determine the working current density. The equilibrium potential of copper in the electrolyte was 0.1 V *vs.* SSCE.

Limiting current density was found to be 120 mA cm^{-2}. However, limiting current densities are never applied for metal deposition due to the formation of low-quality deposits with powder inclusions. The working current density was selected to be half of the limiting – 65 mA cm^{-2}, which gives the deposition rate of 85 μm h^{-1}.

Deposited copper is shown in Figure 4. It can be seen that the surface of the deposited metal is not smooth and dark inclusions can be observed.

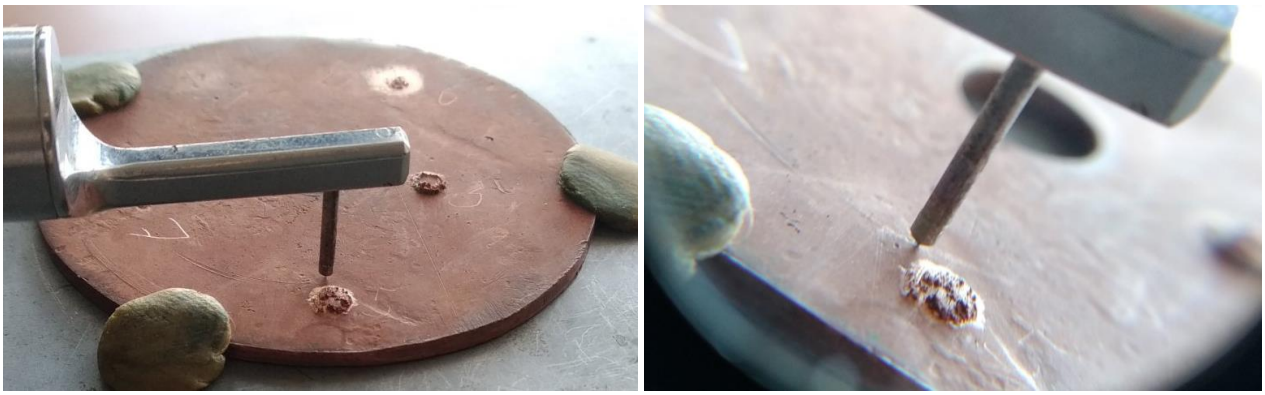

Figure 4. *Locally deposited copper on the surface of copper plate during 3D-profilometry*

The measured profile of the deposited copper and the comparison of the modeled and experimentally deposited copper are given in Figure 5. The profile of the deposited copper shows that the average height agrees well with the COMSOL computer model.

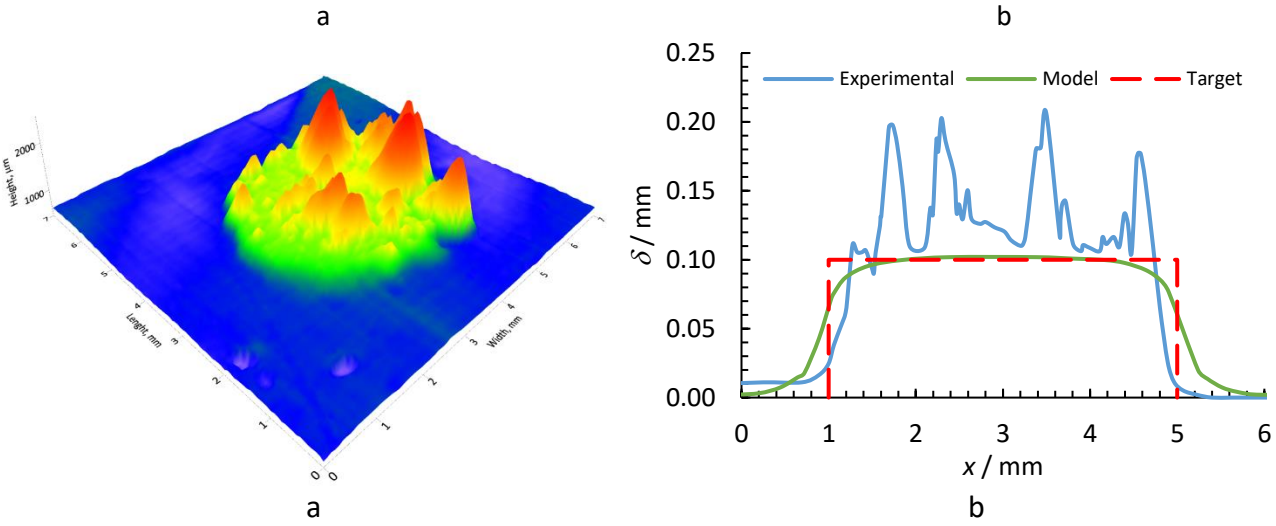

Figure 5. *3D-vizualization of the deposited copper (a) and comparison of deposited, modelled and target profiles of copper (b)*

The side surface of the profile obtained in the experiment is even more straight than in model. However, some areas on the top of the deposited copper demonstrate the presence of peaks, which makes the surface rough. These peaks result from anodic sludge inclusion in the deposits and deposition of copper dendrites. The lower the sulfate acid content in the electrolyte, the lower is copper deposition overvoltage that leads to the formation of dendrites. Also, the dendrite formation may be caused by monovalent copper ions reproportion described by equation (4). Cu^+ ions are formed by staged copper anodic dissolution. This process is known to stimulate the increase of roughness and dendrites formation.

$$2Cu^+ = Cu + Cu^{2+} \quad (4)$$

In the experiment, the soluble anode was used, and the sludge was able to detach from the anode and fall on the surface, where it was grown in the copper. To avoid the inclusions of anodic sludge in the deposited metal and reproportion of copper in further studies, the insoluble anode will be used, and copper overvoltage will be increased using organic additives.

Conclusions

COMSOL computer model is adequate and can be used to select preferable electrolyte conductivity, determine interelectrode gap and predict current distribution during local electrochemical deposition of metals. In the present study the conductivity was 50 mS cm^{-1}, IEG - 5 mm.

The deposited copper profile was found in good agreement with the model. The thickness of the metal layer was 0.1 mm, and the diameter 4 mm, which agrees with the model.

The inclusions of the anodic sludge and dendrites formation were responsible for the surface roughness of the deposited copper. The use of insoluble anode and prevention of dendrites formation in further studies would be preferable to prevent sludge formation.

Acknowledgements: *The work was supported by the Ministry of Science and Education of Ukraine, grant number 2514, 2022.*

References

[1] C. Korner, *International Materials Reviews* **61** (2016) 361-377. https://doi.org/10.1080/09506608.2016.1176289

[2] P. Regenfuss, A. Streek, L. Hartwig, S. Klotzer, Th. Brabant, M. Horn, R. Ebert, H. Exner, *Rapid Prototyping Journal* **13(4)** (2007) 204-212. https://doi.org/10.1108/13552540710776151
[3] L. Xinchao, M. Pingmei, A. Sansan, W. Wei, *International Journal of Machine Tools and Manufacture* **173** (2021) 103848. https://doi.org/10.1016/j.ijmachtools.2021.103848
[4] S. D. Leith, D. T. Schwartz, *Journal of Microelectromechanical Systems* **8(4)** (1999) 384-392. https://doi.org/10.1109/84.809052
[5] A .L. Cohen, U. Frodis, F. G. Tseng, G. Zhang, M. Florian, P. M. Will, *Micromachining and Microfabrication Process Technology V* **3874** (1999) 236-247. https://doi.org/10.1117/12.361227
[6] A. L. Cohen, G. Zhang, F. G. Tseng, F. Mansfield, U. Frodis, P.M. Will, International Solid Freeform Fabrication Symposium, EFAB: batch production of functional, fully-dense metal parts with micron-scale features, Austin, USA, 1998, p. 161-168. https://doi.org/10.26153/tsw/590
[7] J. D. Madden, S. R. Lafontaine, I.W. Hunter, *Sixth International Symposium on Micro Machine and Human Science,* Fabrication by electrodeposition: building 3D structures and polymer actuators, Nagoya, Japan, 1995, pp. 77-81. https://doi.org/10.1109/MHS.1995.494221
[8] J. Xu, W. Ren, Z. Lian, P. Yu, H. Yu, *The International Journal of Advanced Manufacturing Technology* **110** (2020) 1731-1757. https://doi.org/10.1007/s00170-020-05799-5
[9] P. Hanekamp, W. Robl, F.-M. Matysik, *Journal of Applied Electrochemistry* **47** (2017) 1305-1312. https://doi.org/10.1007/s10800-017-1124-8
[10] S. Morsali, S. Daryadel, Z. Zhou, A. Behroozfar, D. Qian, M. Minary-Jolandan, *Journal of Applied Physics* **121** (2017) 024903-024908. https://doi.org/10.1063/1.4973622
[11] H. Fan, Y.P. Zhao, S.K. Wang, *Key Engineering Materials* **667** (2016) 259-264. https://doi.org/10.4028/www.scientific.net/KEM.667.259
[12] J. Hu, M.F. Yu, *Science* **329** (2010) 313-316. https://doi.org/10.1126/science.1190496
[13] S. K. Seol, D. Kim, S. Lee, J. H. Kim, W. S. Chang, J. T. Kim, *Small* **11(32)** (2015) 3896-3902. https://doi.org/10.1002/smll.201500177
[14] A. Behroozfar, S. Daryadel, S. R. Morsali, S. Moreno, M. Baniasadi, R. A. Bernal, M. Minary-Jolanda, *Advanced Materials* **30(4)** (2017) 1705107. https://doi.org/10.1002/adma.201705107
[15] P. Liu, Y. Guo, Y. Wu, J. Chen, Y. Yang, *Crystals* **10(4)** (2020) 257. https://doi.org/10.3390/cryst10040257
[16] K. Nakazawa, M. Yoshioka, Y. Mizutani, T. Ushiki, F. Iwata, *Microsystem Technologies* **26** (2020) 1333-1342. https://doi.org/10.1007/s00542-019-04665-z
[17] G. Ercolano, C. van Nisselroy, T. Merle, J. Vörös, D. Momotenko, W. W. Koelmans, T. Zambelli, *Micromachines* **11(1)** (2020) 6. https://doi.org/10.3390/mi11010006
[18] O. V. Linyucheva, M. I. Donchenko, D. Yu. Ushchapovskiy, M. V. Byk, D. M. Skladanniy, *Eastern-European Journal of Enterprise Technologies* **6** (2014) 48-55. https://doi.10.15587/1729-4061.2014.30660